

FOSTER: Feature Boosting and Compression for Class-Incremental Learning

Fu-Yun Wang, Da-Wei Zhou, Han-Jia Ye, and De-Chuan Zhan

State Key Laboratory for Novel Software Technology, Nanjing University
`wangfuyun@smail.nju.edu.cn, {zhoudw, yehj, zhandc}@lamda.nju.edu.cn`

Abstract. The ability to learn new concepts continually is necessary in this ever-changing world. However, deep neural networks suffer from catastrophic forgetting when learning new categories. Many works have been proposed to alleviate this phenomenon, whereas most of them either fall into the stability-plasticity dilemma or take too much computation or storage overhead. Inspired by the gradient boosting algorithm to gradually fit the residuals between the target and the current approximation function, we propose a novel two-stage learning paradigm FOSTER, empowering the model to learn new categories adaptively. Specifically, we first dynamically expand new modules to fit the residuals of the target and the original model. Next, we remove redundant parameters and feature dimensions through an effective distillation strategy to maintain the single backbone model. We validate our method FOSTER on CIFAR-100, ImageNet-100/1000 under different settings. Experimental results show that our method achieves state-of-the-art performance.

Keywords: class-incremental learning, gradient boosting

1 Introduction

The real world is constantly changing, and new concepts and categories will gradually emerge [16,57,55]. Retraining a model every time new classes emerge is impractical due to data privacy [6] and expensive training costs. Therefore, it is essential to enable the model to continuously learn new categories, namely class-incremental learning [40,53,58,54]. However, directly fine-tuning the model on new data causes a severe problem known as catastrophic forgetting [12] that the model entirely and abruptly forgets previously learned information. Inspired by this, class-incremental learning aims to design a learning paradigm that enables the model to continuously learn novel categories in multiple stages while maintaining the original discriminative ability of old classes.

In recent years, many approaches have been proposed from different aspects. So far, the most widely recognized and utilized class-incremental learning strategy is based on knowledge distillation [21]. Methods [33,40,2,45,52,56] retain an old model additionally and use knowledge distillation to constrain output for original tasks of the new model to be similar to that of the old one [33]. However, the single backbone model may not have enough plasticity [19] to cope with the

coming new categories. Besides, even with restrictions of KD, the model still suffer from feature degradation [47] of old concepts due to limited access [6] to old data. Recently, methods [47,34,10] based on dynamic architectures achieve state-of-the-art performance in class-incremental learning. They preserve old modules with their parameters frozen to maintain the discriminative ability for old categories and expand new trainable modules to strengthen plasticity for learning new categories. Nevertheless, they have two inevitable defects: First, constantly expanding new modules for new tasks will lead to a drastic increase in the number of parameters, resulting in severe storage and computation overhead, which makes these methods not suitable for long-term incremental learning. Second, since old modules have never seen new concepts, retaining them directly may harm performance on new categories. The more old modules kept, the more remarkable the negative impact.

In this paper, we propose a novel perspective to achieve the goal of class-incremental learning. In the scenario of class-incremental learning, distributions of new categories are constantly coming, but the old model can not directly handle new distributions since it has never seen them. The distribution drift will lead to the mismatch between the model output and the target, which is called residual. Inspired by the idea of gradually adding new classifiers to fit the residual between the target and the original model in gradient boosting, we do not update the old model directly on the new data but freeze it and create a new model to fit the residual when new task comes. This new model has positive significance in two aspects: On the one hand, with sufficient new training data, this new model will help the model to learn to distinguish between new classes. Given that the original model can handle old classes well, combining the two will form a strong classifier for both new and old classes [30]. On the other hand, training the new model to classify all categories, including both the new and old concepts, may contribute to discovering some critical elements ignored by the original model. As shown in Fig. 1, when the model learns old categories, including tigers, cats, and monkeys, it may think that stripes are essential information but mistakenly regard auricles as meaningless features. When learning new categories, because the fish and birds do not have auricles, the new model will discover this mistake and correct it. However, creating new models not only leads to an increase in the number of parameters but also causes redundant feature dimensions and inconsistency between the old and the new model. Therefore, we are supposed to further compress the ensemble model to remove unnecessary and inconsistent features, thus preserving crucial information and enhancing the robustness of the model.

To achieve this, we design a new learning paradigm for class-incremental learning based on feature boosting [13] and compression [31]. To this end, our paradigm can be decoupled into two steps. The first step can be seen as boosting to alleviate the performance decline due to the arrival of new classes. Specifically, we retain the old model with all its parameters frozen. Then we expand a trainable new feature extractor and concatenate it with the extractor of the old model and initialize a constrained, fully-connected layer to transform the super

feature into logits. Thus, the logits of all categories can be represented by combining these two feature extractors, which we will demonstrate later in detail. In the second step, we aim to eliminate redundant parameters and meaningless dimensions caused by feature boosting. To achieve this goal, we propose an effective distillation strategy that can transfer knowledge from the boosting model to a single model with negligible performance loss, even if the data is limited when learning new tasks. Extensive experiments on three benchmarks, including CIFAR-100, ImageNet-100/1000 show that our method **Feature BoOSTing and ComprEssion for class-incRemental learning (FOSTER)** obtains the state-of-the-art performance.

2 Related Work

Many works have been done to analyze the reasons for performance degradation in class-incremental learning and alleviate this phenomenon. In this section, we will briefly discuss these methods.

Parameter Regularization. EWC [27], MAS [1], SI [49] add parameter regularization to penalize the parameter drift from the old model. These methods expect small changes in important parameters, thus maintaining the discriminative ability for old categories. The main difference among them is how the importance of parameters is defined. However, all of them are based on some assumptions and simplifications. For example, EWC uses Laplace Approximation and assumes all parameters are independent, while it is often not true.

Knowledge Distillation. Knowledge distillation [21] aims to transfer dark knowledge [28] from the teacher to the student by encouraging the outputs of the student model to approximate the outputs of the teacher model [33]. LwF [33] retains an old model additionally and applies a modified cross-entropy loss to constrain the outputs for old categories of the new model to preserve the capability of the old one. Bic [45], WA [52] propose effective strategies to alleviate the bias of the classifier caused by imbalanced training data after distillation.

Rehearsal. The rehearsal strategy enables the model to have partial access to old data. [40,45,52] allocate a memory to store exemplar instances of previous tasks for replay when learning tasks. [24] preserves low dimensional features instead of instances to reduce the storage overhead. In [46], instances of old categories are synthesized by a generative model [18] for rehearsal. [37] test various exemplar selection strategies, and the results show that different ways of exemplar selection do have a significant impact on performance and herding surpass other strategies in most settings.

Dynamic Architectures. Many works [11,17,23,42,44] have proposed creating new modules to handle the growing training distribution [48,32] dynamically. However, an accurate task id, which is usually unavailable in real-life, is needed for most of these approaches to help them choose the corresponding id-specific module. Recently, methods [47,34,10] successfully apply the dynamic architectures into class incremental learning where the task id is not available, showing their advantages over the single backbone methods. However, as we illustrate

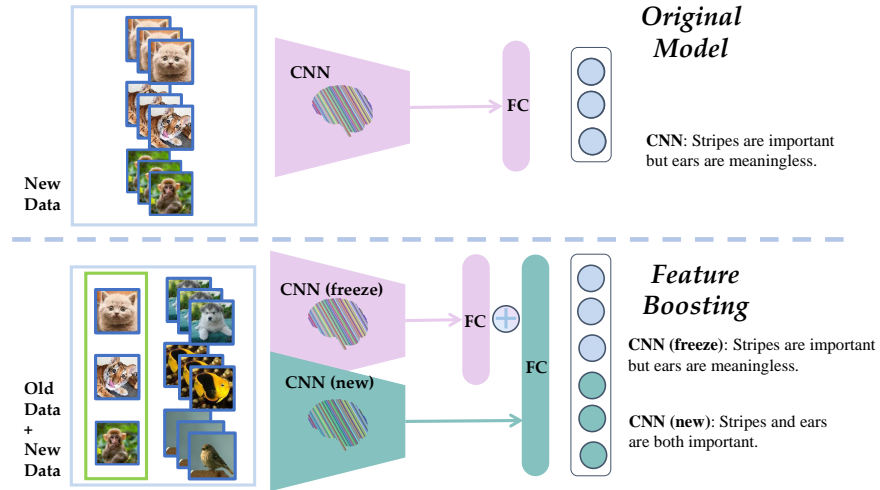


Fig. 1: **Feature Boosting.** Illustration of feature boosting framework. When the task comes, we freeze the original model and create a new module to fit the residual between the target and the original output. The new module helps the model learn both new and old classes better.

in Sec. 1, they have two unavoidable shortcomings: (i) Continual adding new modules causes unaffordable storage and computation overhead. (ii) Directly retaining old modules leads to noise in the feature representation of new categories, harming the performance of new classes.

Boosting. Boosting represents a family of machine learning algorithms that convert weak learners to strong ones [59]. AdaBoost [14] is one of the most famous boosting algorithms, aiming to minimize the exponential loss of the additive model. The crucial idea is to adjust the weights of samples to make the new base learner pay more attention to instances that the former models cannot recognize correctly. In recent years, gradient boosting [15] based algorithms [4,26,8] achieve excellent performance on various tasks.

3 Preliminary

Ensemble algorithms based on gradient boosting have achieved great success in the past few years. In this section, we briefly discuss the basic process of gradient boosting. In Sec. 4, we will demonstrate how we apply the gradient boosting algorithm to class-incremental learning.

3.1 Baseline For Gradient Boosting

[38] illustrates that gradient boosting algorithms can be viewed as iterative functional gradient descent algorithms. Namely, gradient boosting algorithms choose

a weak hypothesis in each step to converge and find the ideal hypothesis that gradually minimizes the cost function.

Particularly, given a training set $\mathcal{D}_{train} = \{(x_i, y_i)\}_{i=1}^n$, the gradient boosting method seeks a hypothesis \hat{F} to minimize the empirical risk

$$\hat{F} = \arg \min_{F} \mathbb{E}_{(x,y) \in \mathcal{D}_{train}} [\ell(y, F(x))], \quad (1)$$

by iteratively adding a new weighted weak function $h_i(x)$ from hypothesis space \mathcal{H}_i . After m stages, \hat{F} can be represented as

$$\hat{F}(x) = F_m(x) = \sum_{i=1}^m \alpha_i h_i(x). \quad (2)$$

In order to find F_{m+1} for further optimization of the cost function, we should optimize the following formula:

$$F_{m+1}(x) = F_m(x) + \arg \min_{h_{m+1} \in \mathcal{H}_{m+1}} \mathbb{E}_{(x,y) \in \mathcal{D}_{train}} [\ell(y, F_m(x) + h_{m+1}(x))]. \quad (3)$$

However, directly optimizing the above function to find the best h_{m+1} is typically infeasible. The idea is to apply the steepest descent step to optimize this problem iteratively, which can be written as

$$F_{m+1}(x) = F_m(x) - \alpha_m \nabla_{F_m} \mathbb{E}_{(x,y) \in \mathcal{D}_{train}} [\ell(y, F_m(x))], \quad (4)$$

where $-\alpha_m \nabla_{F_m} \mathbb{E}_{(x,y) \in \mathcal{D}_{train}} [\ell(y, F_m(x))]$ is the objective for $h_{m+1}(x)$ to approximate. Specifically, if $\ell(\cdot, \cdot)$ is the mean-squared error (MSE), the objective can be represented by

$$-\nabla_{F_m} \mathbb{E}_{(x,y) \in \mathcal{D}_{train}} [(y - F_m(x))^2] = 2 \times \mathbb{E}_{(x,y) \in \mathcal{D}_{train}} [y - F_m(x)], \quad (5)$$

which is the average residual of y and $F_m(x)$ on \mathcal{D}_{train} . Ideally, let $\alpha_m = 1/2$, if $h_{m+1}(x)$ can fit $2\alpha_m(y - F_m(x)) = (y - F_m(x))$ for each $(x, y) \in \mathcal{D}_{train}$, F_{m+1} is the optimal function, minimizing the empirical error.

4 Method

In this section, we give a description of our method and how it works to prompt the model to simultaneously learn both old and new classes well with limited data and parameters.

Below, we first describe the setting of class-incremental learning in Sec. 4.1. After that, we give a full demonstration of how the idea of the gradient boosting algorithm can be applied to class-incremental learning to achieve the trade-off between stability and plasticity. Then we propose novel strategies to alleviate the bias of classification caused by limited access to old data in Sec. 4.3. Finally, in order to avoid the explosive growth of parameters and remove redundant parameters and feature dimensions, we use a straightforward and effective compression method based on knowledge distillation in Sec. 4.4.

4.1 Class-Incremental Learning Setup

Unlike the traditional case where the model is trained on all classes with all training data available, in class-incremental learning, the model receives a batch of new training data $\mathcal{D}_t = \{(\mathbf{x}_i^t, y_i^t)\}_{i=1}^n$ in the t^{th} stage. Specifically, n is the number of training samples, $\mathbf{x}_i^t \in \mathcal{X}_t$ is the input image, and $y_i^t \in \mathcal{Y}_t$ is the corresponding label for \mathbf{x}_i^t . Label space of all seen categories is denoted as $\hat{\mathcal{Y}}_t = \bigcup_{i=0}^t \mathcal{Y}_i$, where $\mathcal{Y}_t \cap \mathcal{Y}_{t'} = \emptyset$ for $t \neq t'$. In the t^{th} stage, rehearsal-based methods also save a part of old data as \mathcal{V}_t , a limited subset of $\bigcup_{i=0}^{t-1} \mathcal{D}_i$. Our model is trained on $\hat{\mathcal{D}}_t = \mathcal{D}_t \cup \mathcal{V}_t$ and is required to perform well on all seen categories.

4.2 From Gradient Boosting to Class-Incremental Learning

Assuming in the t^{th} stage, we have saved the model \mathbf{F}_{t-1} from the last stage. \mathbf{F}_{t-1} can be further decomposed into feature embedding and linear classifier: $\mathbf{F}_{t-1}(\mathbf{x}) = (\mathbf{W}_{t-1})^\top \Phi_{t-1}(\mathbf{x})$, where $\Phi_{t-1}(\cdot) : \mathbb{R}^D \rightarrow \mathbb{R}^d$ and $\mathbf{W}_{t-1} \in \mathbb{R}^{d \times |\hat{\mathcal{Y}}_{t-1}|}$. When a new data stream comes, directly fine-tuning \mathbf{F}_{t-1} on the new data will impair its capacity for old classes, which is inadvisable. On the other hand, simply freezing \mathbf{F}_{t-1} causes it to lose plasticity for new classes, making the residual between target y and $\mathbf{F}_{t-1}(\mathbf{x})$ large for $(\mathbf{x}, y) \in \mathcal{D}_t$. Inspired by gradient boosting, we train a new model to fit the residual. Specifically, the new model \mathcal{F}_t consists of a feature extractor $\phi_t(\cdot) : \mathbb{R}^D \rightarrow \mathbb{R}^d$ and a linear classifier $\mathcal{W}_t \in \mathbb{R}^{d \times |\hat{\mathcal{Y}}_t|}$. \mathcal{W}_t can be further decomposed into $[\mathcal{W}_t^{(o)}, \mathcal{W}_t^{(n)}]$, where $\mathcal{W}_t^{(o)} \in \mathbb{R}^{d \times |\hat{\mathcal{Y}}_{t-1}|}$ and $\mathcal{W}_t^{(n)} \in \mathbb{R}^{d \times |\mathcal{Y}_t|}$. The training process can be represented as

$$\mathbf{F}_t(\mathbf{x}) = \mathbf{F}_{t-1}(\mathbf{x}) + \arg \min_{\mathcal{F}_t} \mathbb{E}_{(\mathbf{x}, y) \in \hat{\mathcal{D}}_t} [\ell(y, \mathbf{F}_{t-1}(\mathbf{x}) + \mathcal{F}_t(\mathbf{x}))]. \quad (6)$$

Similar to Sec. 3.1, let $\ell(\cdot, \cdot)$ be the mean-squared error function, considering the strong feature representation learning ability of neural networks, we expect $\mathcal{F}_t(\mathbf{x})$ can fit residual of y and $\mathbf{F}_{t-1}(\mathbf{x})$ for every $(\mathbf{x}, y) \in \hat{\mathcal{D}}_t$:

$$\begin{aligned} \mathbf{y} &= \mathbf{F}_t(\mathbf{x}) \\ &= \mathbf{F}_{t-1}(\mathbf{x}) + \mathcal{F}_t(\mathbf{x}) \\ &= \mathcal{S} \left(\begin{bmatrix} \mathbf{W}_{t-1}^\top \\ \mathbf{O} \end{bmatrix} \Phi_{t-1}(\mathbf{x}) \right) + \mathcal{S} \left(\begin{bmatrix} (\mathcal{W}_t^{(o)})^\top \\ (\mathcal{W}_t^{(n)})^\top \end{bmatrix} \phi_t(\mathbf{x}) \right), \end{aligned} \quad (7)$$

where $\mathcal{S}(\cdot)$ is the softmax operation, $\mathbf{O} \in \mathbb{R}^{d \times |\mathcal{Y}_t|}$ is set to zero matrix or fine-tuned on $\hat{\mathcal{D}}_t$ with Φ_{t-1} frozen, and \mathbf{y} is the corresponding one-hot vector of y . We set \mathbf{O} to zero matrix as default in our discussion.

Denote the parameters of \mathcal{F}_t as θ_t , this process can be represented as the following optimization problem:

$$\theta_t^* = \arg \min_{\theta_t} \left\| \mathbf{y} - \left\{ \mathcal{S} \left(\begin{bmatrix} \mathbf{W}_{t-1}^\top \\ \mathbf{O} \end{bmatrix} \Phi_{t-1}(\mathbf{x}) \right) + \mathcal{S} \left(\begin{bmatrix} (\mathcal{W}_t^{(o)})^\top \\ (\mathcal{W}_t^{(n)})^\top \end{bmatrix} \phi_t(\mathbf{x}) \right) \right\} \right\|_1.$$

To simplify implementation, we replace the sum of softmax with softmax of logits sum and substitute the mean-absolute error (MAE) with the Kullback-Leibler divergence (KLD), then the objective function changes into:

$$\begin{aligned}\theta_t^* &= \arg \min_{\theta_t} \text{KL}(y \parallel F_t(\mathbf{x})) \\ &= \arg \min_{\theta_t} \text{KL}\left(y \parallel \mathcal{S}\left(\begin{bmatrix} \mathbf{W}_{t-1}^\top (\mathcal{W}_t^{(o)})^\top \\ \mathbf{O} (\mathcal{W}_t^{(n)})^\top \end{bmatrix} \begin{bmatrix} \Phi_{t-1}(\mathbf{x}) \\ \phi_t(\mathbf{x}) \end{bmatrix}\right)\right).\end{aligned}\quad (8)$$

Therefore, F_t can be represented as an expanded linear classifier \mathbf{W}_t and a concatenated super feature extractor $\Phi_t(\cdot)$, where

$$\mathbf{W}_t^\top = \begin{bmatrix} \mathbf{W}_{t-1}^\top (\mathcal{W}_t^{(o)})^\top \\ \mathbf{O} (\mathcal{W}_t^{(n)})^\top \end{bmatrix} \quad (9)$$

$$\Phi_t(\mathbf{x}) = \begin{bmatrix} \Phi_{t-1}(\mathbf{x}) \\ \phi_t(\mathbf{x}) \end{bmatrix}. \quad (10)$$

Note that \mathbf{W}_{t-1}^\top , \mathbf{O} , and Φ_{t-1} are all frozen, the trainable modules are the $\phi_t, \mathcal{W}_t^{(o)}, \mathcal{W}_t^{(n)}$. Here we explain their roles. Logits of F_t is

$$\mathbf{W}_t^\top \Phi_t(\mathbf{x}) = \begin{bmatrix} \mathbf{W}_{t-1}^\top \Phi_{t-1}(\mathbf{x}) + (\mathcal{W}_t^{(o)})^\top \phi_t(\mathbf{x}) \\ (\mathcal{W}_t^{(n)})^\top \phi_t(\mathbf{x}) \end{bmatrix}. \quad (11)$$

The upper part is the logits of old classes, and the lower part is the logits of new ones. The lower part requires the new module \mathcal{F}_t to learn how to correctly classify new classes, thus enhancing the model's plasticity to redeem the performance on new classes. The upper part encourages the new module to fit the residual between y and F_{t-1} . Note that the final output probabilities are computed with softmax of both old and new categories, and thus the increase of classes facilitates the discovery of crucial information ignored by F_{t-1} .

4.3 Calibration for Old and New

In incremental learning scenarios, our training set $\hat{\mathcal{D}}_t = \mathcal{D}_t \cup \mathcal{V}_t$ is imbalanced. That is to say, we can get sufficient data of new categories from \mathcal{D}_t , but only a small part of old data is available from \mathcal{V}_t due to storage cost and privacy problems. The long-tail distribution of \mathcal{D}_t will result in a strong classification bias in the model [25, 52, 45, 2]. To alleviate the classification bias and encourage the model to equally learning old and new classes, we illustrate Logits Alignment and Feature Enhancement strategies in the following sections.

Logits Alignment. To strengthen the learning of old instances and mitigate the classification bias, we add a scale factor to the logits of the old and new classes in Equation. 11 respectively during training. Thus, the logits during training are:

$$\gamma \mathbf{W}_t^\top \Phi_t(\mathbf{x}) = \begin{bmatrix} \gamma_1 (\mathbf{W}_{t-1}^\top \Phi_{t-1}(\mathbf{x}) + (\mathcal{W}_t^{(o)})^\top \phi_t(\mathbf{x})) \\ \gamma_2 (\mathcal{W}_t^{(n)})^\top \phi_t(\mathbf{x}) \end{bmatrix}, \quad (12)$$

where $0 < \gamma_1 < 1$, $\gamma_2 > 1$, and γ is a diagonal matrix composed of γ_1 and γ_2 . Through this scaling strategy, the absolute value of logits for old categories is reduced and the absolute value of logits for new ones is enlarged, thus forcing the model F_t to produce larger logits for old categories and smaller logits for new categories.

We get γ_1, γ_2 through normalized effective number E_n [5] of each class as its scale factor:

$$E_n = \begin{cases} \frac{1-\beta^n}{1-\beta}, & \beta \in [0, 1) \\ n, & \beta = 1 \end{cases}, \quad (13)$$

concretely, $(\gamma_1, \gamma_2) = \left(\frac{E_{n_{\text{old}}}}{E_{n_{\text{old}}} + E_{n_{\text{new}}}}, \frac{E_{n_{\text{new}}}}{E_{n_{\text{old}}} + E_{n_{\text{new}}}} \right)$. Hence the loss function is formulated as:

$$\mathcal{L}_{LA} = \text{KL}(y \parallel \mathcal{S}(\gamma \mathbf{W}_t^\top \Phi_t(\mathbf{x}))). \quad (14)$$

Feature Enhancement. We argue that simply letting a new module $\mathcal{F}_t(\mathbf{x})$ fit the residual of $F_{t-1}(\mathbf{x})$ and label y is sometimes insufficient. At one extreme, for instance, the residual of $F_{t-1}(\mathbf{x})$ and y is zero. In that case, the new module \mathcal{F}_t can not learn anything about old categories, and thus it will damage the performance of our model for old classes. Hence, we should prompt the new module \mathcal{F}_t to learn old categories further.

Our Feature Enhancement consists of two parts. First, we initialize a new linear classifier $\mathbf{W}_t^{(a)} \in \mathbb{R}^{d \times |\hat{\mathcal{Y}}_t|}$ to transform the new feature $\phi_t(\mathbf{x})$ into logits of all seen categories and require the new feature itself to correctly classify all of them:

$$\mathcal{L}_{FE} = \text{KL}(y \parallel \mathcal{S}((\mathbf{W}_t^{(a)})^\top \phi_t(\mathbf{x}))). \quad (15)$$

Hence, even if the residual of $F_{t-1}(\mathbf{x})$ and y is zero, the new feature extractor ϕ_t can still learn how to classify the old categories. Besides, it should be noted that simply using one-hot targets to train the new feature extractor in an imbalanced dataset might lead to overfitting to small classes, failing to learn a feature representation with good generalization ability for old categories. To alleviate this phenomenon and provide more supervision for old classes, we utilize knowledge distillation to encourage $F_t(\mathbf{x})$ to have similar output distribution as F_{t-1} on old categories.

$$\mathcal{L}_{KD} = \text{KL}(\mathcal{S}(F_{t-1}(\mathbf{x})) \parallel \mathcal{S}(F_{t-1}(\mathbf{x}) + (\mathcal{W}_t^{(o)})^\top \phi_t(\mathbf{x}))) \quad (16)$$

Note that this process requires only one more time matrix multiplication computation because the forward process of the original model F_{t-1} and the expanded model F_t is shared, except for the final linear classifier.

Summary of Feature Boosting. To conclude, feature-boosting consists of three components. First, we create a new module to fit the residual between targets and the output of the original model, following the principle of gradient boosting. With reasonable simplification and deduction, the optimization

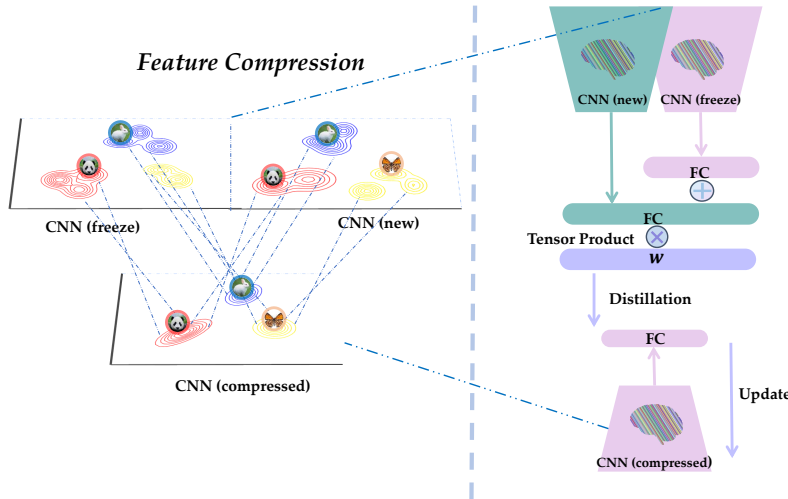


Fig. 2: **Feature Compression.** Left: the process of feature compression. We remove insignificant dimensions and parameters to make the distribution of the same categories more compact. Right: the implementation of feature compression. Outputs of the dual branch model are used to instruct the representation learning of the single backbone model. Different weights are assigned to old and new classes to alleviate the classification bias.

objective is transformed into the minimization of KL divergence of the target and the output of the concatenated model. To alleviate the classification bias caused by imbalanced training, we proposed logits alignment (LA) to balance the training of old and new classes. Moreover, we argued that simply letting the new module fit the residual is sometimes insufficient. To further encourage the new module to learn old instances, we proposed feature enhancement, where \mathcal{L}_{FE} aims to make the new module learn the difference among all categories by optimizing the cross-entropy loss of target and the output of the new module, and \mathcal{L}_{KD} utilize the original output to instruct the expanded model through knowledge distillation. The final FOSTER loss for boosting combines the above three components:

$$\mathcal{L}_{Boosting} = \mathcal{L}_{LA} + \mathcal{L}_{FE} + \mathcal{L}_{KD}. \quad (17)$$

4.4 Feature Compression

Our method FOSTER achieves excellent performance through gradient boosting. However, gradually adding new modules \mathcal{F} to our model F_t will lead to the growing number of parameters and feature dimensions of our model F_t , making it unable to be applied in long-term incremental learning. There is an interesting question here. Do we really need so many parameters and feature dimensions?

For example, we create the same module \mathcal{F} to learn tasks with 2 classes and 50 classes and achieve similar effects. Thus, there must be redundant parameters and meaningless feature dimensions in the task with 2 classes. Inspired by the feature selection and dimension reduction in the traditional machine learning paradigm, are we able to compress the expanded feature space of F_t to a much smaller feature space with almost no performance degradation?

Knowledge distillation [21] is a simple yet effective way to achieve this goal. Since our model F_t can handle all seen categories with excellent performance, it can give any input a soft target, namely the output distribution on all known categories. Therefore, except for the current training set $\hat{\mathcal{D}}_t$, we can sample other unlabeled data from a similar domain for further distillation. Note that these unlabeled data can be obtained from the Internet during distillation and discarded after that, so it does not occupy additional memory.

Here, we do not expect additional auxiliary data is available and find that with simple strategies, we can achieve remarkable performance with only an imbalanced dataset $\hat{\mathcal{D}}_t$.

Balanced Distillation. Suppose there is a single backbone student model $F_t^{(s)}$ to be distilled. To mitigate the classification bias caused by imbalanced training dataset $\hat{\mathcal{D}}_t$, we should consider the class priors and adjust the weights of distilled information for different classes [51]. Therefore, the Balanced Distillation loss is formulated as:

$$\mathcal{L}_{\text{BKD}} = \text{KL}\left(\mathbf{w} \otimes \mathcal{S}(F_t(\mathbf{x})) \parallel \mathcal{S}(F_t^{(s)}(\mathbf{x}))\right), \quad (18)$$

where \otimes means the tensor product and \mathbf{w} is the weighted vector obtained from Eq. 13 to make classes with fewer instances have larger weights. To further strengthen the learning of old categories, we also mixup [50] exemplars of old categories in the same mini-batch and add them into the batch for training.

5 Experiments

In this section, we compare our FOSTER with other state-of-the-art methods on benchmark incremental learning datasets. We also conduct ablations to validate the effectiveness of each component in FOSTER.

5.1 Experimental Settings

Datasets. We validate our methods on widely used benchmark of class-incremental learning CIFAR-100 [29] and ImageNet100/1000 [7]. **CIFAR-100:** CIFAR-100 consists of 50,000 training images with 500 images per class, and 10,000 testing images with 100 images per class. **ImageNet-1000:** ImageNet-1000 is a large scale dataset composed of about 1.28 million images for training and 50,000 for validation with 500 images per class. **ImageNet-100:** ImageNet-100 is composed of 100 classes randomly chosen from the original ImageNet-1000.

Protocol. For both the CIFAR-100 and ImageNet-100, we validate our method on two widely used protocols: (i) **CIFAR-100/ImageNet-100 B0 (base 0):** In

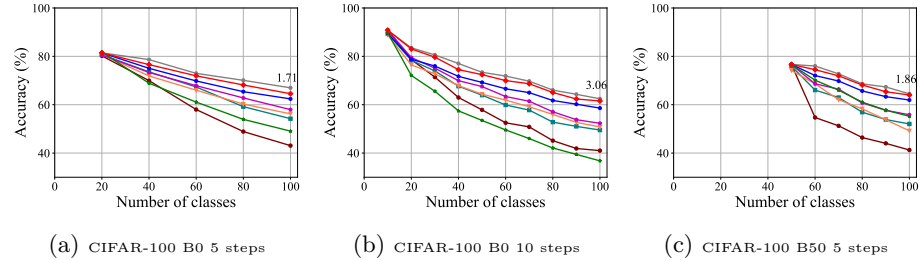


Fig. 3: **Incremental Accuracy on CIFAR-100.** Replay is the baseline with only rehearsal strategy. FOSTER B4 records the accuracy of the dual branch model after feature boosting in each step. FOSTER records the accuracy of the single backbone model after feature compression.

Table 1: Average incremental accuracy on CIFAR-100 for FOSTER vs. state-of-the-art. DER uses the same number of backbone models as incremental sessions, while the other methods, including FOSTER, retain only one backbone model after the end of each session.

Methods	Average accuracy of all sessions (%)			
	B0 10 steps	B0 20 steps	B50 10 steps	B50 25 steps
Bound	80.40	80.41	81.49	81.74
iCaRL [40]	64.42	63.5	53.78	50.60
BiC [45]	65.08	62.37	53.21	48.96
WA [52]	67.08	64.64	57.57	54.10
PODNet [9]	55.22	47.87	63.19	60.72
DER [47]	69.74	67.98	66.36	-
Ours	72.90	70.65	67.95	63.83
Improvement	(+3.06)	(+2.67)	(+1.59)	(+3.11)

the first protocols, we train all 100 classes gradually with 5, 10, 20 classes per step with the fixed memory size of 2,000 exemplars. (ii) **CIFAR-100/ImageNet-100 B50 (base 50):** We also start by training the models on half the classes. Then we train the rest 50 classes with 2, 5, 10 classes per step with 20 examples as memory per class. For ImageNet-1000, we train all 1000 classes with 100 classes per step (10 steps in total) with a fixed memory size of 20,000.

Implementation Details. Our method and all compared methods are implemented with Pytorch [39]. The code will be made publicly available. For ImageNet, we adopt the standard ResNet-18 [20] as our feature extractor and set the batch size to 256. The learning rate starts from 0.1 and gradually decays to zero with a cosine annealing scheduler [35] (170 epochs in total). For CIFAR-100, we use a modified ResNet-32 [40] as the most previous works as our feature extractor and set the batch size to 128. The learning rate also starts from 0.1 and gradually decays to zero with a cosine annealing scheduler (170 epochs in total). For both ImageNet and CIFAR-100, we use SGD with the momentum of 0.9 and the weight decay of 5e-4 in the boosting stage. In the compression stage, we use SGD with the momentum of 0.9 and set the weight decay to 0. We set the temperature scalar T to 2. The hyperparameter β to compute the effective

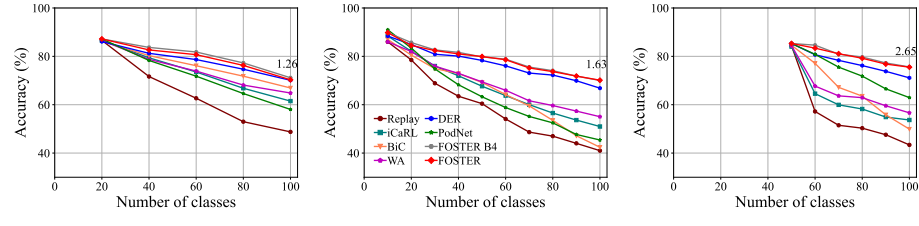


Fig. 4: **Incremental Accuracy on ImageNet-100.** Replay is the baseline with only rehearsal strategy. FOSTER B4 records the accuracy of the dual branch model after feature boosting in each step. FOSTER records the accuracy of the single backbone model after feature compression.

number is set to 0.97 in most settings. We use herding as our default strategy to sampling exemplars.

5.2 Quantitative results

CIFAR-100. Table 1 and Fig. 3 summarize the results of CIFAR100 benchmark. We use replay as the baseline method, which only uses rehearsal strategy to alleviate forgetting. Experimental results show that our method outperforms the other state-of-the-art strategies in all six settings on CIFAR100. Our method achieves excellent performance on both long-term incremental learning tasks and large step incremental learning tasks. Particularly, we achieve 3.11% and 2.67% improvement under the long-term incremental setting of base 50 with 25 steps and base 0 with 20 steps, respectively. We also surpass the state-of-the-art method by 1.71% and 3.06% under the large step incremental learning setting of 20 classes per step and 10 classes per step. It should also be noted that although our method FOSTER expands a new module every time, we compress it to a single backbone every time. Therefore, the parameters and feature dimensions of our model do not increase with the number of tasks, which is our advantage over methods [47,34,10] based on dynamic architecture. From Fig. 3, we can also see that the single backbone model FOSTER after feature compression has a tiny gap with FOSTER B4 in each step, which verifies the effectiveness of our distillation method.

ImageNet. Table 2 and Fig. 4 summarize the experimental results for ImageNet-100 and ImageNet-1000 benchmarks. Our method FOSTER, still outperforms the other method in most settings. In the setting of ImageNet-100 B0, we surpass the state-of-the-art method by 1.26, 1.63, and 0.7 percent points for respectively 5, 10, and 20 steps. The results shown in Fig. 4 again verify the effectiveness of our distillation strategy, where the performance degradation after compression is negligible. The results on ImageNet-1000 benchmark is shown in the right-most column in Tabel 2. Our method improves the average top-1 accuracy on ImageNet-1000 with 10 steps from 66.73% to 68.34% (+1.61%), showing that our method is also efficacious in large-scale incremental learning.

Table 2: Average incremental accuracy on ImageNet for FOSTER vs. state-of-the-art. DER uses the same number of backbone models as incremental sessions, while the other methods, including FOSTER, retain only one backbone model after the end of each session. The left three columns are experimental results on ImageNet-100. The rightmost column is the results of ImageNet-1000 with 100 classes per step (10 steps in total).

Methods	Average accuracy of all sessions (%)			
	B0 20 steps	B50 10 steps	B50 25 steps	ImageNet-1000
Bound	81.20	81.20	81.20	89.27
iCaRL [40]	62.36	59.53	54.56	38.4
BiC [45]	58.93	65.14	59.65	-
WA [52]	63.2	63.71	58.34	54.10
PODNet [9]	53.69	74.33	67.28	-
DER [47]	73.79	77.73	-	66.73
Ours	74.49	77.54	69.34	68.34
Improvement	(+0.7)	(-0.19)	(+2.06)	(+1.61)

5.3 Ablation Study

Different Components of FOSTER. Table 5 demonstrates the results of our ablative experiments on CIFAR100 B50 with 5 steps. Specifically, we replace logits alignments (LA) with the post-processing method weight alignment (WA) [52]. The performance comparison is shown in Fig. 5a, where LA surpasses WA by about 4% in the final accuracy. This shows that our LA is a more efficacious strategy than WA in calibration for old and new classes. We remove feature enhancement and compare its performance with the original result in Fig. 5b, the model suffers from more than 3% performance decline in the last stage. We also find that, in the last step, there is almost no difference in the accuracy of new classes between the model with feature enhancement and the model without that. Nevertheless, the model with feature enhancement outperforms the model without that by more than 4 % on old categories, showing that feature enhancement encourages the model to learn more about old categories. We compare the performance of balanced knowledge distillation (BKD) with that of normal knowledge distillation (KD) in Fig. 5c. BKD surpasses KD in all stages, showing that BKD is more suitable for class incremental learning due to the imbalanced dataset.

Sensitive Study of Hyper-parameters. To verify the robustness of our method, we conduct experiments on CIFAR-100 B50 5 steps with different hyperparameters $\beta \in (0, 1)$. Usually, β is set more than 0.9. Therefore, we test $\beta = 0.93, 0.95, 0.97, 0.99, 0.995, 0.999$ respectively. The experimental results are shown in Fig. 6a. From the results, we can see that the performance changes are minimal under different β , which verifies that our method has good robustness to hyperparameters.

Effect of Number of Exemplars. In Fig. 6b, We gradually increase the number of exemplars from 5 to 200 and record the performance of the model on cifar100 B50 with 5 steps. The accuracy in the last step increases from 53.53%

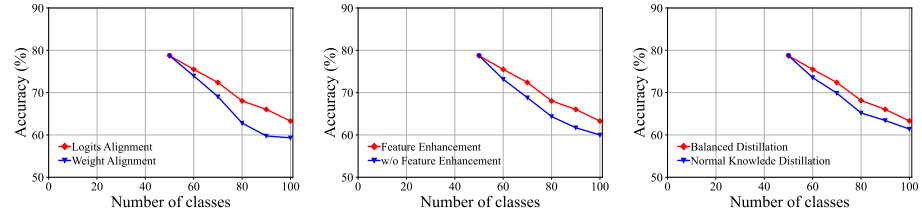


Fig. 5: **Ablations** of the different key components of FOSTER. (a): Performance comparison between logits alignment and weight alignment [52]. (b): Performance comparison with or without Feature Enhancement. (c): Performance comparison between balanced distillation and normal knowledge distillation [21].

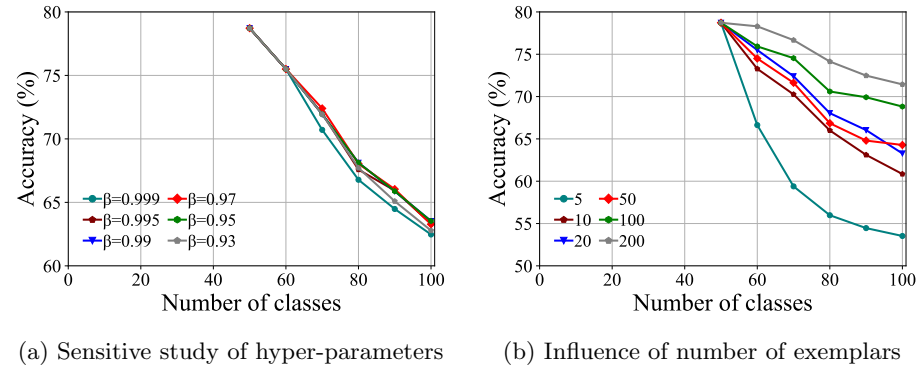


Fig. 6: **Robustness testing.** Left: Performance under different hyperparameters. Right: Performance with different numbers of exemplars. Both of them are evaluated on CIFAR-100 B50 with 5 steps.

to 71.4% as the number of exemplars for every class changes from 5 to 200. From the results, we can see that with the increase of the number of exemplars, the accuracy of the last stage of the model gradually improves, indicating that our model can make full use of more exemplars to improve performance. In addition, notice that our model achieves more than 60% accuracy in the last round, even when there are only 10 exemplars for each class, surpassing most state-of-the-art methods using 20 exemplars shown in Fig. 3c. This indicates that our approach is more effective and robust; it can still overcome forgetting even if the number of exemplars is small.

6 Conclusions

In this work, we apply the gradient boosting algorithm to class-incremental learning and propose a novel learning paradigm FOSTER, empowering the model to learn new categories adaptively. At each step, we create a new module to learn residuals between the target and the original model. We also introduce logits alignment to alleviate classification bias and feature enhancement to balance the

representation learning of the old and new classes. We also propose a simple yet effective distillation strategy to remove redundant parameters and dimensions, compressing the expanded model into its original size. Extensive experiments on three widely used incremental learning benchmarks show that our method obtains state-of-the-art performance.

References

1. Aljundi, R., Babiloni, F., Elhoseiny, M., Rohrbach, M., Tuytelaars, T.: Memory aware synapses: Learning what (not) to forget. In: ECCV. pp. 139–154 (2018)
2. Castro, F.M., Marín-Jiménez, M.J., Guil, N., Schmid, C., Alahari, K.: End-to-end incremental learning. In: ECCV. pp. 233–248 (2018)
3. Chai, T., Draxler, R.R.: Root mean square error (rmse) or mean absolute error (mae)?—arguments against avoiding rmse in the literature. *Geoscientific model development* **7**(3), 1247–1250 (2014)
4. Chen, T., Guestrin, C.: Xgboost: A scalable tree boosting system. In: KDD. pp. 785–794 (2016)
5. Cui, Y., Jia, M., Lin, T.Y., Song, Y., Belongie, S.: Class-balanced loss based on effective number of samples. In: CVPR. pp. 9268–9277 (2019)
6. Delange, M., Aljundi, R., Masana, M., Parisot, S., Jia, X., Leonardis, A., Slabaugh, G., Tuytelaars, T.: A continual learning survey: Defying forgetting in classification tasks. *IEEE Transactions on Pattern Analysis and Machine Intelligence* (2021)
7. Deng, J., Dong, W., Socher, R., Li, L.J., Li, K., Fei-Fei, L.: Imagenet: A large-scale hierarchical image database. In: CVPR. pp. 248–255. Ieee (2009)
8. Dorogush, A.V., Ershov, V., Gulin, A.: Catboost: gradient boosting with categorical features support. *arXiv preprint arXiv:1810.11363* (2018)
9. Douillard, A., Cord, M., Ollion, C., Robert, T., Valle, E.: Podnet: Pooled outputs distillation for small-tasks incremental learning. In: ECCV. pp. 86–102. Springer (2020)
10. Douillard, A., Ramé, A., Couairon, G., Cord, M.: Dytox: Transformers for continual learning with dynamic token expansion. *arXiv preprint arXiv:2111.11326* (2021)
11. Fernando, C., Banarse, D., Blundell, C., Zwols, Y., Ha, D., Rusu, A.A., Pritzel, A., Wierstra, D.: Pathnet: Evolution channels gradient descent in super neural networks. *arXiv preprint arXiv:1701.08734* (2017)
12. French, R.M.: Catastrophic forgetting in connectionist networks. *Trends in cognitive sciences* **3**(4), 128–135 (1999)
13. Freund, Y., Schapire, R., Abe, N.: A short introduction to boosting. *Journal-Japanese Society For Artificial Intelligence* **14**(771-780), 1612 (1999)
14. Friedman, J., Hastie, T., Tibshirani, R.: Additive logistic regression: a statistical view of boosting (with discussion and a rejoinder by the authors). *The annals of statistics* **28**(2), 337–407 (2000)
15. Friedman, J.H.: Greedy function approximation: a gradient boosting machine. *Annals of statistics* pp. 1189–1232 (2001)
16. Golab, L., Özsü, M.T.: Issues in data stream management. *ACM Sigmod Record* **32**(2), 5–14 (2003)
17. Golkar, S., Kagan, M., Cho, K.: Continual learning via neural pruning. *arXiv preprint arXiv:1903.04476* (2019)
18. Goodfellow, I., Pouget-Abadie, J., Mirza, M., Xu, B., Warde-Farley, D., Ozair, S., Courville, A., Bengio, Y.: Generative adversarial nets. *Advances in neural information processing systems* **27** (2014)
19. Grossberg, S.: Adaptive resonance theory: How a brain learns to consciously attend, learn, and recognize a changing world. *Neural networks* **37**, 1–47 (2013)
20. He, K., Zhang, X., Ren, S., Sun, J.: Deep residual learning for image recognition. In: CVPR. pp. 770–778 (2016)
21. Hinton, G., Vinyals, O., Dean, J., et al.: Distilling the knowledge in a neural network. *arXiv preprint arXiv:1503.02531* **2**(7) (2015)

22. Hu, Z., Hong, L.J.: Kullback-leibler divergence constrained distributionally robust optimization. Available at Optimization Online pp. 1695–1724 (2013)
23. Hung, C.Y., Tu, C.H., Wu, C.E., Chen, C.H., Chan, Y.M., Chen, C.S.: Compact-ing, picking and growing for unforgetting continual learning. Advances in Neural Information Processing Systems **32** (2019)
24. Iscen, A., Zhang, J., Lazebnik, S., Schmid, C.: Memory-efficient incremental learning through feature adaptation. In: ECCV. pp. 699–715. Springer (2020)
25. Kang, B., Xie, S., Rohrbach, M., Yan, Z., Gordo, A., Feng, J., Kalantidis, Y.: Decoupling representation and classifier for long-tailed recognition. arXiv preprint arXiv:1910.09217 (2019)
26. Ke, G., Meng, Q., Finley, T., Wang, T., Chen, W., Ma, W., Ye, Q., Liu, T.Y.: Lightgbm: A highly efficient gradient boosting decision tree. Advances in neural information processing systems **30** (2017)
27. Kirkpatrick, J., Pascanu, R., Rabinowitz, N., Veness, J., Desjardins, G., Rusu, A.A., Milan, K., Quan, J., Ramalho, T., Grabska-Barwinska, A., et al.: Overcoming catastrophic forgetting in neural networks. Proceedings of the national academy of sciences **114**(13), 3521–3526 (2017)
28. Korattikara Balan, A., Rathod, V., Murphy, K.P., Welling, M.: Bayesian dark knowledge. Advances in Neural Information Processing Systems **28** (2015)
29. Krizhevsky, A., Hinton, G., et al.: Learning multiple layers of features from tiny images (2009)
30. Krogh, A., Vedelsby, J.: Neural network ensembles, cross validation, and active learning. Advances in neural information processing systems **7** (1994)
31. Kumar, V., Minz, S.: Feature selection: a literature review. SmartCR **4**(3), 211–229 (2014)
32. Lesort, T., Caselles-Dupré, H., Garcia-Ortiz, M., Stoian, A., Filliat, D.: Generative models from the perspective of continual learning. In: IJCNN. pp. 1–8. IEEE (2019)
33. Li, Z., Hoiem, D.: Learning without forgetting. IEEE transactions on pattern analysis and machine intelligence **40**(12), 2935–2947 (2017)
34. Li, Z., Zhong, C., Liu, S., Wang, R., Zheng, W.S.: Preserving earlier knowledge in continual learning with the help of all previous feature extractors. arXiv preprint arXiv:2104.13614 (2021)
35. Loshchilov, I., Hutter, F.: Sgdr: Stochastic gradient descent with warm restarts. arXiv preprint arXiv:1608.03983 (2016)
36. Van der Maaten, L., Hinton, G.: Visualizing data using t-sne. Journal of machine learning research **9**(11) (2008)
37. Masana, M., Liu, X., Twardowski, B., Menta, M., Bagdanov, A.D., van de Weijer, J.: Class-incremental learning: survey and performance evaluation on image classification. arXiv preprint arXiv:2010.15277 (2020)
38. Mason, L., Baxter, J., Bartlett, P., Frean, M.: Boosting algorithms as gradient descent. Advances in neural information processing systems **12** (1999)
39. Paszke, A., Gross, S., Chintala, S., Chanan, G., Yang, E., DeVito, Z., Lin, Z., Desmaison, A., Antiga, L., Lerer, A.: Automatic differentiation in pytorch (2017)
40. Rebuffi, S.A., Kolesnikov, A., Sperl, G., Lampert, C.H.: icarl: Incremental classifier and representation learning. In: CVPR. pp. 2001–2010 (2017)
41. Rubinstein, R.Y., Kroese, D.P.: The cross-entropy method: a unified approach to combinatorial optimization, Monte-Carlo simulation, and machine learning, vol. 133. Springer (2004)
42. Rusu, A.A., Rabinowitz, N.C., Desjardins, G., Soyer, H., Kirkpatrick, J., Kavukcuoglu, K., Pascanu, R., Hadsell, R.: Progressive neural networks. arXiv preprint arXiv:1606.04671 (2016)

43. Serra, J., Suris, D., Miron, M., Karatzoglou, A.: Overcoming catastrophic forgetting with hard attention to the task. In: ICML. pp. 4548–4557. PMLR (2018)
44. Wen, Y., Tran, D., Ba, J.: Batchensemble: an alternative approach to efficient ensemble and lifelong learning. arXiv preprint arXiv:2002.06715 (2020)
45. Wu, Y., Chen, Y., Wang, L., Ye, Y., Liu, Z., Guo, Y., Fu, Y.: Large scale incremental learning. In: CVPR. pp. 374–382 (2019)
46. Wu, Z., Baek, C., You, C., Ma, Y.: Incremental learning via rate reduction. In: CVPR. pp. 1125–1133 (2021)
47. Yan, S., Xie, J., He, X.: Der: Dynamically expandable representation for class incremental learning. In: CVPR. pp. 3014–3023 (2021)
48. Yoon, J., Yang, E., Lee, J., Hwang, S.J.: Lifelong learning with dynamically expandable networks. arXiv preprint arXiv:1708.01547 (2017)
49. Zenke, F., Poole, B., Ganguli, S.: Continual learning through synaptic intelligence. In: ICML. pp. 3987–3995. PMLR (2017)
50. Zhang, H., Cisse, M., Dauphin, Y.N., Lopez-Paz, D.: mixup: Beyond empirical risk minimization. In: ICLR (2018)
51. Zhang, S., Chen, C., Hu, X., Peng, S.: Balanced knowledge distillation for long-tailed learning. arXiv preprint arXiv:2104.10510 (2021)
52. Zhao, B., Xiao, X., Gan, G., Zhang, B., Xia, S.T.: Maintaining discrimination and fairness in class incremental learning. In: CVPR. pp. 13208–13217 (2020)
53. Zhou, D.W., Wang, F.Y., Ye, H.J., Ma, L., Pu, S., Zhan, D.C.: Forward compatible few-shot class-incremental learning. arXiv preprint arXiv:2203.06953 (2022)
54. Zhou, D.W., Wang, F.Y., Ye, H.J., Zhan, D.C.: Pycil: A python toolbox for class-incremental learning. arXiv preprint arXiv:2112.12533 (2021)
55. Zhou, D.W., Yang, Y., Zhan, D.C.: Learning to classify with incremental new class. IEEE Transactions on Neural Networks and Learning Systems (2021)
56. Zhou, D.W., Ye, H.J., Zhan, D.C.: Co-transport for class-incremental learning. In: ACM MM. pp. 1645–1654 (2021)
57. Zhou, D.W., Ye, H.J., Zhan, D.C.: Learning placeholders for open-set recognition. In: CVPR (2021)
58. Zhou, D.W., Ye, H.J., Zhan, D.C.: Few-shot class-incremental learning by sampling multi-phase tasks. arXiv preprint arXiv:2203.17030 (2022)
59. Zhou, Z.H.: Ensemble methods: foundations and algorithms. CRC press (2012)

Supplementary Material

I Rationality Analysis of Simplified Implementation.

We argue that our simplification of replacing the sum of softmax with softmax of logits sum and substituting the mean-absolute error (MAE) with the Kullback-Leibler divergence (KLD).

MAE is used to evaluate the residual between the target and the output. However, MAE is hard to optimize numerically [3] and is unsuitable for classification tasks. Similar to MAE, KLD can also evaluate the residual between the target and the output by calculating the distance between the target label distribution and the output distribution of categories. KLD is more suitable for classification tasks and there are some works [22,41] that point out that the KLD has many advantages in many aspects, including faster optimization and better feature representation.

Typically, to reflect the relative magnitude of each output, we use non-linear activation softmax to transform the output logits into the output probability. Namely, $p_1, p_2, \dots, p_{|\hat{\mathcal{Y}}_t|}$, where $0 \leq p_i \leq 1$, $\sum_{i=1}^{|\hat{\mathcal{Y}}_t|} p_i = 1$ and $|\hat{\mathcal{Y}}_t|$ is the number of all seen categories. In classification tasks, the target label is usually set to 1 and the non-target label is set to 0. Therefore, we expect the output of the boosting model can be constrained between 0 and 1. Simply combining the softmax outputs of the original model F_{t-1} and \mathcal{F}_t can not satisfy the constraints. Suppose that the output of F_{t-1} and \mathcal{F}_t in class i are p_i^o and p_i^n , the combination of p_i^n and p_i^o is not in line with our expectation since $0 \leq p_i^o + p_i^n \leq 2$. By replacing the sum of softmax with softmax of logits sum, we can limit the output of the boosting model between 0 and 1, and the judgment of the two models can still be integrated.

II The Influence of the Initialization of the Weight \mathbf{O}

In this section, we discuss the effect of the initialization of the weight \mathbf{O} in the super linear classifier of our boosting model.

$$\mathbf{W}_t^\top = \begin{bmatrix} \mathbf{W}_{t-1}^\top (\mathcal{W}_t^{(o)})^\top \\ \mathbf{O} (\mathcal{W}_t^{(n)})^\top \end{bmatrix}. \quad (1)$$

In the main paper, we set \mathbf{O} to all zero as our default initialization strategy. Therefore, the outputs of the original model for new categories are zero, thus having nothing to do with the classification of new classes.

Here, we introduce three different initialization strategies, including fine-tune (FT), all-zero (AZ), and all-zero with bias (AZB), to further explore the impact of different initialization strategies on performance. Among them, FT is directly training \mathbf{O} without any restrictions. AZ sets the outputs of the old model on the new class to all zero, and thus the outputs of the model on the

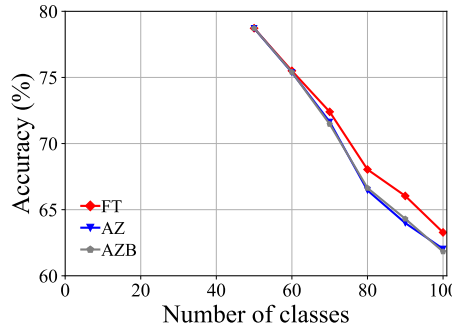


Fig. 1: **Influence of different initialization strategies.** The red line represents FT, the blue line represents AZ, and the gray line represents AZB. The performance of FT is slightly better than AZ and AZB. The performance gap between AZ and AZB is negligible.

new class logits only contain the output of the new model, the old model does not provide any judgment on the new class. On the basis of AZ, AZB adds bias learning to balance the logits of the old and new categories. Fig. 1 illustrates the comparison of performance on CIFAR-100 [29] B50 with 5 steps with different initialization strategies. We can see that the performance of using FT initialization strategy is slightly better than that of using AZ and AZB initialization strategies, but the difference is not significant. The performance gap between AZ and AZB is negligible, indicating that the influence of bias is weak.

III Introduction about Compared Methods

In this section, we will describe in detail the methods compared in the main paper.

Fine-tune: Fine-tune is the baseline method that simply updates its parameters when a new task comes, suffering from catastrophic forgetting. By default, weights corresponding to the outputs of previous classes in the final linear classifier are not updated.

Replay: Replay utilizes rehearsal strategy to alleviate the catastrophic forgetting compared to Fine-tune. We use herding as the default way of choosing exemplars from the old data.

iCaRL [40]: iCaRL combines cross-entropy loss with knowledge distillation loss together. It retains an old model to help the new model maintain the discriminative ability through knowledge distillation on old categories. To mitigate the classification bias caused by the imbalanced dataset when learning new tasks, iCaRL calculates the center of exemplars for each category and uses NME as the classifier for evaluation.

BiC [45]: BiC performs an additional bias correction process compared to iCaRL, retaining a small validation set to estimate the classification bias resulting from imbalanced training. The final logits are computed by

$$q_k = \begin{cases} o_k & 1 \leq k \leq n \\ \alpha o_k + \beta & n+1 \leq k \leq n+m \end{cases}, \quad (2)$$

where n is the number of old categories and m is the number of new ones. the bias correction step is to estimate the appropriate α and β .

WA [52]: During the process of incremental learning, the norms of the weight vectors of new classes are much larger than those of old classes. Based on that, WA proposes an approach called Weight Alignment to correct the biased weights in the final classifier by aligning the norms of the weight vectors of new classes to those of old classes.

$$\widehat{\mathbf{W}}_{new} = \gamma \cdot \mathbf{W}_{new}, \quad (3)$$

where $\gamma = \frac{\text{Mean}(\mathbf{Norm}_{old})}{\text{Mean}(\mathbf{Norm}_{new})}$.

PODNet [9]: PODNet proposes a novel spatial-based distillation loss that can be applied throughout the model. PODNet has greater performance on long runs of small incremental tasks.

DER [47]: DER preserves old feature extractors to maintain knowledge for old categories. When new tasks come, DER creates a new feature extractor and concatenates it with old feature extractors to form a higher dimensional feature space. In order to reduce the number of parameters, DER uses the pruning method proposed in HAT [43], but the number of parameters still increases with the number of tasks. DER can be seen as a particular case of our Boosting model, when we set the weight \mathbf{O} of boosting model can be trainable, and remove feature enhancement and logits alignment proposed in the main paper, boosting model can be reduced to DER.

IV Visualization of Detailed Performance

Visualizing Feature Representation. We visualize the feature representations of the test data by t-SNE [36]. Fig. 2 illustrates the comparison of baseline method, fine-tune, with our FOSTER in the setting of CIFAR-100 [29] B50 with 5 steps. As shown in Fig. 2a and Fig. 2g, in the base task, all categories can form good clusters with explicit classification boundaries. However, as shown in Fig. 2b, Fig. 2c, Fig. 2d, Fig. 2e, and Fig. 2f, in stages of incremental learning, the result of category clustering becomes very poor without clear classification boundaries. In the last stage which is shown in Fig. 2f, feature points of each category are scattered. On the contrary, as shown in Fig. 2g, Fig. 2h, Fig. 2i, Fig. 2j, Fig. 2k, and Fig. 2l, our FOSTER method can make all categories form good clusters at each incremental learning stage, and has a clear classification boundary, indicating that our FOSTER method is a very effective strategy in feature representation learning and overcoming catastrophic forgetting.

Visualizing Confusion Matrix. To compare with other methods, we visualize the confusion matrices of different methods at the last stage in Fig. 3. In these confusion matrices, the vertical axis represents the real label, and the horizontal axis represents the label predicted by the model. Warmer colors indicate higher prediction rates, and cold colors indicate lower prediction rates. Therefore, the warmer the point color on the diagonal, the colder the color on the other points, the better the performance of the model. Fig. 3a shows the confusion matrix of fine-tune. The brightest colors on the right and colder colors elsewhere suggest that the fine-tune method has a strong classification bias, tending to classify inputs into new categories and suffering from severe catastrophic forgetting. Fig. 3b shows the confusion matrix of iCaRL [40]. iCaRL has obvious performance improvement compared with fine-tune. However, the columns on the right are still bright, indicating that they also have a strong classification bias. In addition, the points on the diagonal have obvious discontinuities, indicating that they cannot make all categories achieve a good accuracy. Fig. 3c shows the confusion matrices of WA [52]. Benefiting from Weight Alignment, WA significantly reduces classification bias compared with iCaRL. The rightmost columns have no obvious brightness. But its accuracy on old classes is not high enough. As shown in the figure, most of his color brightness at the diagonal position of the old class is between 0.2 and 0.4. Fig. 3d shows the confusion matrices of DER [47]. DER achieves good results in both old and new categories, but the brightness of the upper right corner shows that it still suffers from classification bias and has room for improvement. As shown in Fig. 3e, our method FOSTER performs well in all categories and well balances the accuracy of the old and new classes.

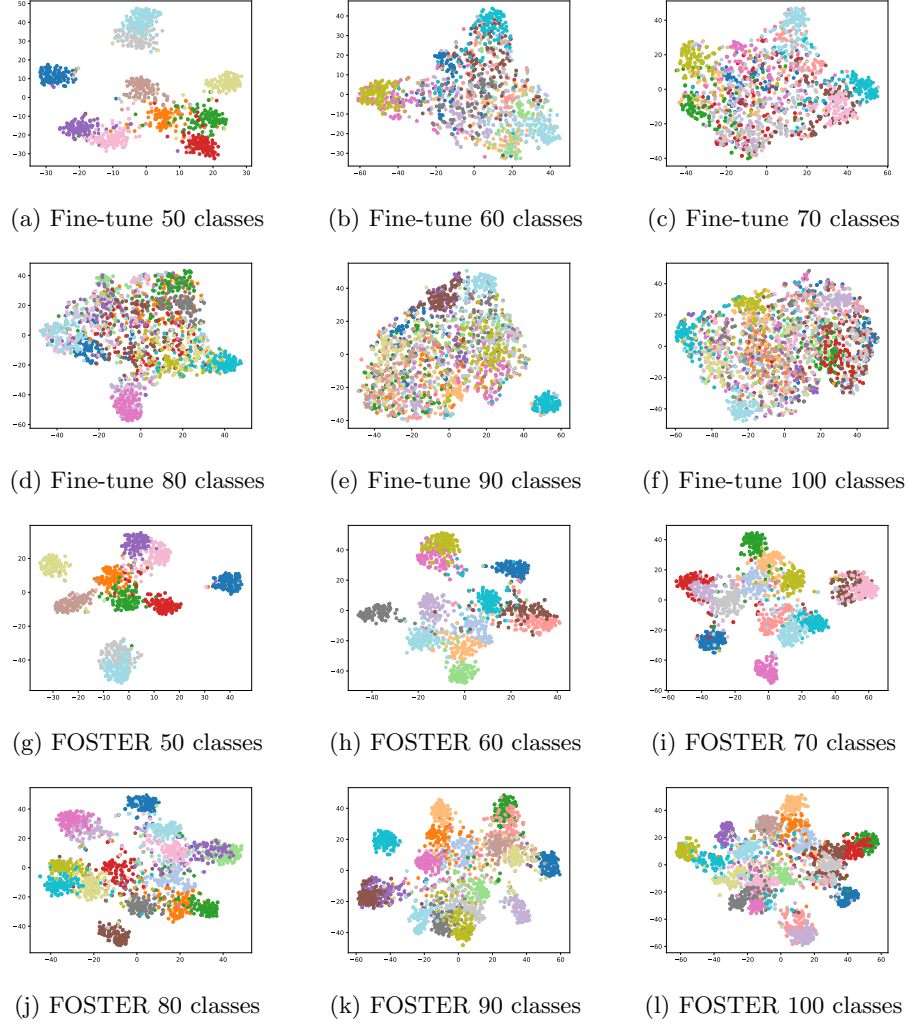


Fig. 2: t-SNE [36] visualization of CIFAR-100 [29] B50 with 5 steps. Figure (a)-(g) shows the t-SNE visualization of fine-tune method. Figure (h)-(l) shows the t-SNE visualization of our method FOSTER. **In order to achieve better results, we normalize each feature and randomly select one category in each five categories for visualization.**

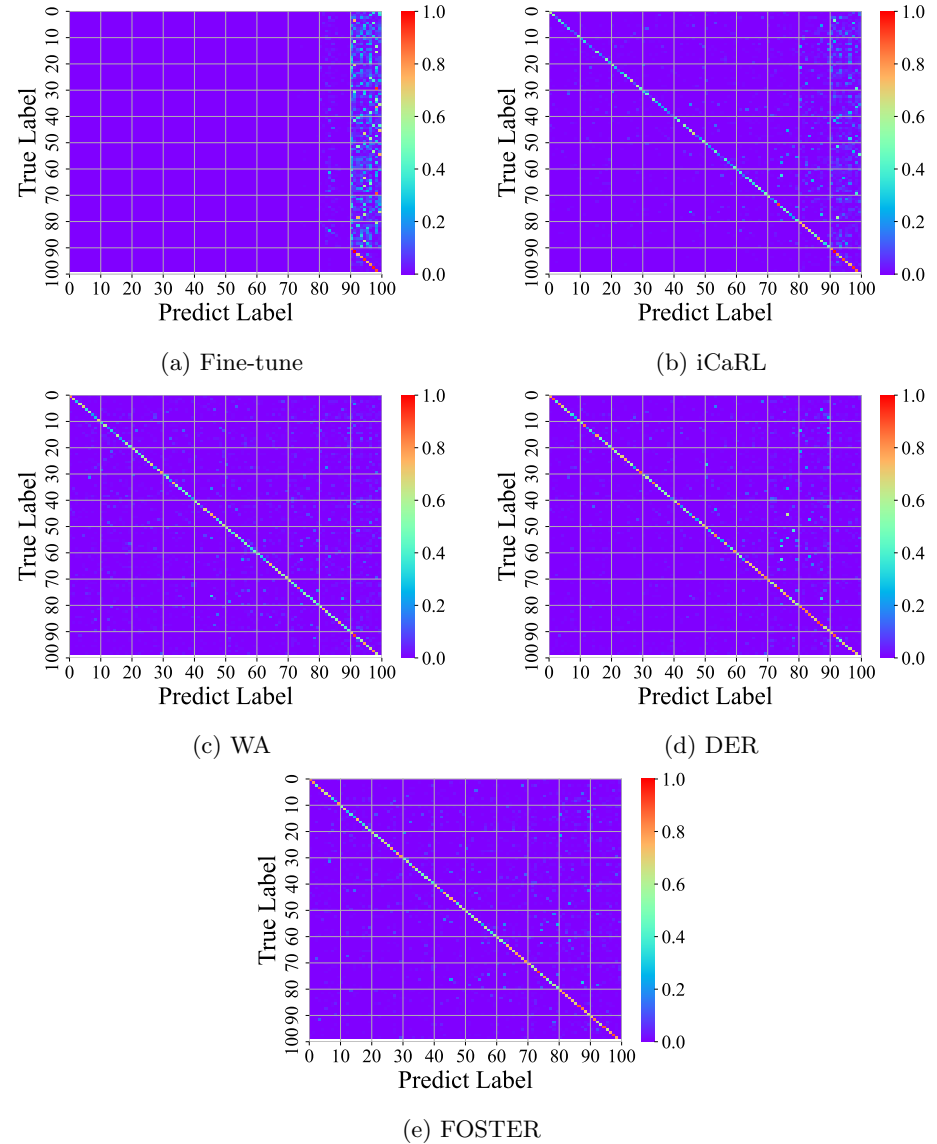


Fig. 3: **Confusion matrices of different methods.** The vertical axis represents the real label, and the horizontal axis represents the label predicted by the model. The warmer the color of a point in the graph, the more samples it represents.